

shown; rather the figure assumes larger  $\Delta$  values to be associated with larger asymmetry parameters. Due to different degrees of distortions observed for both the  $S=PS_{3/2}$  and  $PS_{3/2}$  units, the isotropic chemical shift ranges from these microstructures overlap strongly. Thus, in phosphorus sulfide systems with unknown bond angles or distributions thereof, such microstructures cannot be identified by straightforward isotropic chemical shift comparisons. However, a close inspection of Table I shows that the variation in the S-P-S bonding angles changes primarily  $\theta_{33}$ , whereas the most shielded component  $\delta_{11}$  is virtually unaffected. This is particularly evident from the plot shown for the  $S=PS_{3/2}$  units in Figure 8. Thus, in an analysis of disordered or glassy systems, the presence of such units can be inferred from a unique  $\delta_{11}$  component of ca.  $-50 \pm 10$  ppm. Table I reveals that none of the other microstructures present in the compounds studied here will pose interferences in this spectral region. In addition, Figure 8 suggests that distribution functions for intracage bond angles are available from  $\theta_{33}$ . However, the latter analysis will generally only be possible if the presence of other units, which resonate in the same spectral region, has been excluded.

The limited amount of data available for compounds containing  $PS_{3/2}$  units suggests a similar conclusion as above: The most shielded shift tensor component  $\delta_{11}$  remains virtually unaffected by symmetry distortions. However, in contrast to the  $S=PS_{3/2}$

units, the least shielded shift tensor component decreases with increasing symmetry distortion, leading to a reduction of the overall chemical shift anisotropy. Further work on the different modifications of  $P_4S_4$  and  $P_4S_5$  is in progress in order to elucidate whether the  $\delta_{11}$  tensor component is sufficiently unique to enable a distinction from microstructures that may contain additional phosphorus-phosphorus bonds.

The present work suggests the utility of the anisotropic shielding information preserved in magic-angle spinning-sideband patterns for making structural assignments. The approach taken here differs from the usual approach of emphasizing the isotropic chemical shift information by either fast spinning or sideband suppression techniques. We propose to use this method to identify microstructures in disordered systems such as the non-oxide chalcogenide glasses. Such studies are currently under way in our laboratories.

*Acknowledgment.* Research support from the UCSB academic senate (H.E.) and the Office of Naval Research (G.D.S) is gratefully acknowledged. The 202.49-MHz solid-state NMR studies were carried out at the NSF Regional NMR Facility at the California Institute of Technology.

*Registry No.*  $P_4S_3$ , 1314-85-8;  $P_4S_7$ , 12037-82-0;  $P_4S_9$ , 25070-46-6;  $P_4S_{10}$ , 15857-57-5.

## Effects of Pressure on the Thermal Decomposition Kinetics and Chemical Reactivity of Nitromethane

G. J. Piermarini, S. Block,

*Institute for Materials Science and Engineering, National Bureau of Standards,  
Gaithersburg, Maryland 20899*

and P. J. Miller\*

*Naval Surface Warfare Center, White Oak, Maryland 20910 (Received: January 15, 1988;  
In Final Form: June 22, 1988)*

The effects of pressure and temperature on the melting point, thermal decomposition rate, and chemical reactivity of nitromethane have been studied. A diamond anvil high-pressure cell in conjunction with (1) an optical polarizing microscope for melting point and chemical reactivity observations and (2) an automated Fourier transform infrared instrument for thermal decomposition kinetic measurements was used. Both pressure and temperature were found to increase the rate of thermal decomposition, indicating an overall bimolecular reaction mechanism. However, the mechanism is complex and appears to vary over large changes in pressure. Nevertheless, a chemical mechanism is proposed that explains the bimolecularity and also accounts for the observed decomposition products, ammonium formate and water. A dynamic stress-induced catastrophic reaction in nitromethane, which appears to be crystal orientation dependent with respect to the applied stress, was found. Under the same conditions, deuterated nitromethane did not exhibit this catastrophic reaction.

### Introduction

Recently, we reported the effects of pressure and temperature on the thermal decomposition rate and reaction mechanism of the nitramine HMX ( $\beta$ -octahydro-1,3,5,7-tetranitro-1,3,5,7-tetrazocine).<sup>1</sup> The material was found to thermally decompose in the pressure regime below 6 GPa through primarily a complex unimolecular mechanism in which pressure significantly decreased the rate of the decomposition reaction. At pressures greater than 6 GPa, however, pressure was found to enhance the decomposition rate, and the reaction mechanism appears to cross over to bimolecular character. Those results on HMX were significant because they described, for the first time, the chemistry, kinetics,

and mechanisms of the decomposition of an explosive material at pressures and temperatures corresponding to those characteristic of predetonation conditions.

In the present paper, we report results of similar measurements on nitromethane obtained by the same high-pressure technique. At elevated pressures, the thermal decomposition of nitromethane is expected to behave differently from HMX. Previously reported time-to-explosion measurements on nitromethane up to 5 GPa indicate that pressure decreases the time required to achieve an explosion.<sup>2</sup> As a result of this behavior, pressure is expected to have a similar effect on the thermal decomposition rate in nitromethane, and if this is indeed the case, then the reaction

(1) Piermarini, G. J.; Block, S.; Miller, P. J. *J. Phys. Chem.* **1987**, *91*, 3872.

(2) Lee, E. L.; Sandborn, R. H.; Stromberg, H. D. *Proc. 5th Symp. (Int) Detonation* **1970**, 331.

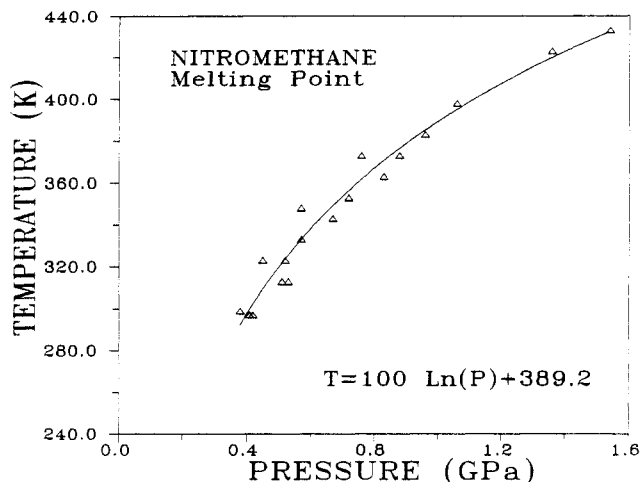


**Figure 1.** Equilibrium melting point of nitromethane as a function of pressure and temperature. The data points were fitted to a logarithmic function of the form indicated in the diagram. The curve was not determined at higher pressures and temperatures than those indicated (1.54 GPa and 433 K), because nitromethane undergoes rapid thermal decomposition above these conditions.

mechanism should be bimolecular in character.

Nitromethane, the simplest of the aliphatic nitro compounds, is an important monopropellant and explosive, i.e., it is a pure compound that reacts at a rate sufficient to provide an impulse and, under the right conditions, a detonation. An understanding of the ignition and burning processes must be based upon a thorough knowledge of the structure and its pressure dependence of the ground and excited states of the molecule, including the means by which intermolecular interactions and energy-transfer processes can occur.

In this paper, we report the pressure and temperature dependencies of the rate of thermal decomposition of nitromethane up to 7 GPa. Through a combination of the measured pressure effects on the thermal decomposition kinetics and the identification of the products of decomposition, we propose a possible bimolecular reaction mechanism for the nitromethane decomposition process.

### Experimental Section

The melting point of nitromethane as a function of pressure and temperature was observed optically with the aid of a polarizing microscope. The instrumentation permitting these observations has been described in detail in previous reports, and, therefore, will not be presented here.<sup>3-5</sup> The two-phase condition (crystal and liquid) can be maintained as the temperature is varied by a corresponding appropriate change in pressure, thereby ensuring that the measurements are made at equilibrium conditions. In this manner, the equilibrium phase boundary between solid and liquid can be delineated over a desired pressure-temperature range. In the case of nitromethane, that range extends to about 1.54 GPa and 433 K as shown in Figure 1. Above these conditions thermal decomposition initiates and is readily observed visually by darkening of the liquid and crystal producing ultimately brown solid residue, liquid, and gases. Upon release of pressure, only the solid residue remains. This residue, which has been retrieved and analyzed in the present experiments by mass spectrometry to determine its chemical constituents, will be discussed in detail later.

The previously described method used to study the effects of pressure on the kinetics of thermal decomposition of HMX<sup>1</sup> was employed in the present nitromethane study. Briefly, the method consists of a diamond anvil high-pressure cell (DAC) specially designed for static heating for temperature up to 1073 K. The DAC, fabricated from a high-temperature high-strength super-

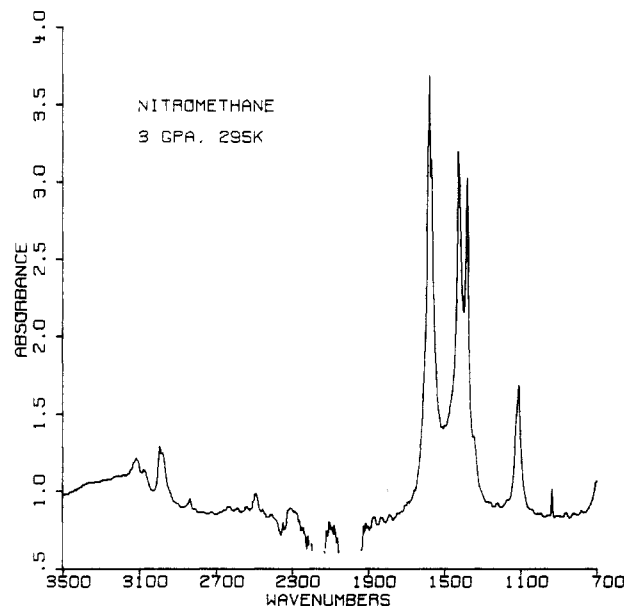


**Figure 2.** Experimental infrared absorbance spectrum of crystalline nitromethane at 3.0 GPa and room temperature obtained with the sample contained in a diamond anvil high-pressure cell. Thin films on the order of 0.3–0.6  $\mu\text{m}$  were required to obtain spectra of this quality.

alloy, inconel 718, is mounted on a micrometer positioning device inside the sample chamber of a Nicolet 7000 FTIR spectrometer equipped with an enhanced MCT (HgCdTe) detector. Protonated and deuterated samples of nitromethane (99% purity) were obtained from Fluka-Garantie, and these liquids were used without further purification.

As in our earlier work, the rate measurements were made by monitoring infrared absorption spectra at various pressures and temperatures as a function of time during the decomposition reaction. The nitromethane sample was prepared as a thin film in a gasketed DAC containing powdered NaCl compacted to transparency, providing both a visible and infrared window approximately 250  $\mu\text{m}$  in diameter. Embedded in the NaCl was a small ruby sphere, approximately 5  $\mu\text{m}$  in diameter, which served as the pressure sensor.<sup>6</sup> The assembled pressure cell, when mounted in the path of the infrared beam, consisted of two opposed diamond anvils (type IIa with low birefringence) separated by an Inconel X750 gasket (250- $\mu\text{m}$  diameter) containing a transparent NaCl window. A thin film of nitromethane placed on the NaCl provided a sample approximately 10  $\mu\text{m}$  thick (estimated from channel spectra) with the plane of the film normal to the direction of the infrared beam. Further details concerning the sample preparation and configuration can be found in ref 5.

A typical rate measurement involved setting the sample pressure at a desired value by using the ruby fluorescence method of pressure measurement.<sup>3,6</sup> A He-Cd laser operating at a maximum continuous wave power of 40 mW was used to excite the ruby fluorescence R lines. The laser beam focused at the sample is approximately 15  $\mu\text{m}$  in diameter, which is roughly the same size as the ruby sphere used as the pressure sensor. No spectral changes were observed in the materials studied or in their decomposition products before or after the pressure measurements, indicating no laser effect on the materials. The DAC containing the sample at pressure was then mounted in the sample chamber of the FTIR spectrometer and heated to the desired decomposition temperature. A kinetics program in the data system was used to collect and store the sequential absorption spectra as a function of time at the desired conditions of pressure and temperature. The scans were monitored by the internal clock of the computer. A typical nitromethane sample required 32 scans (1 s per scan) to yield good spectra with 4- $\text{cm}^{-1}$  resolution over the spectral range 4000–700  $\text{cm}^{-1}$ . It should be noted, however, that as few as 10

(3) Barnett, J. D.; Block, S.; Piermarini, G. J. *Rev. Sci. Instrum.* **1973**, *44*, 1.

(4) Block, S.; Piermarini, G. J. *Phys. Today* **1976**, *29*, 44.

(5) Miller, P. J.; Piermarini, G. J.; Block, S. *Appl. Spectrosc.* **1984**, *38*, 680.

(6) Piermarini, G. J.; Block, S.; Barnett, J. D.; Forman, R. A. *J. Appl. Phys.* **1975**, *46*, 2774.

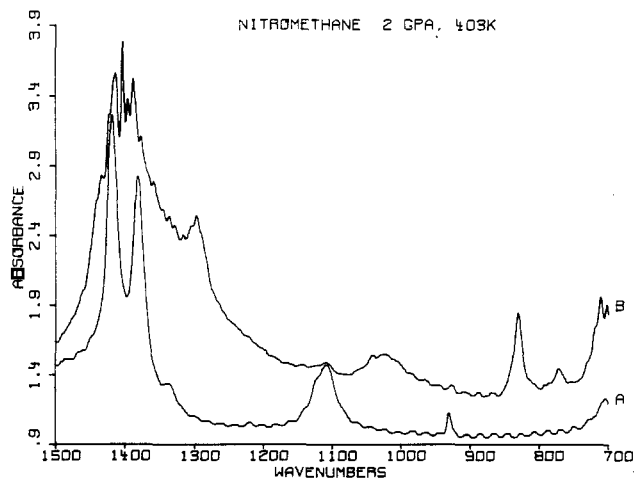


**Figure 3.** Infrared absorbance spectra of nitromethane (A) and thermally decomposed nitromethane (B) with the sample held at 2.0 GPa and 403 K. The limited spectral range shown here serves to identify the major decomposition product bands that have been identified as those arising mainly from ammonium formate. The bands in spectrum B at  $\approx 775$ ,  $\approx 1310$ , and  $\approx 1400$  are due to solid ammonium formate, while the observed bands at  $\approx 825$ ,  $\approx 1030$ , and  $\approx 1100$  result from gaseous products which may include  $N_2O$  and  $CO_2$ .

scans gave spectra with signal-to-noise ratios sufficient for analysis. Infrared absorption spectra were taken up to 7.1 GPa and 453 K. Figure 2 shows a typical absorption spectrum with  $4\text{-cm}^{-1}$  resolution of nitromethane at 3 GPa and room temperature. The infrared absorption spectrum of nitromethane is well-known, and identification of the bands shown here can be found in ref 7 and 8.

Mass spectra analyses were carried out on rapidly decomposed and slowly decomposed nitromethane samples. The samples were introduced by direct-probe and low-resolution electron impact mass spectra at 70 eV were recorded. The probe was initially cooled with ice water to reduce the loss of volatile components. The spectra were recorded as the probe was heated in small increments.

### Experimental Results and Discussion

*Effects of Pressure on the Melting Point and Chemical Reactivity of Nitromethane.* The measured pressure dependence of the equilibrium melting temperature of nitromethane, shown in Figure 1, is logarithmic in this pressure range and can be fitted to the equation

$$T = 100 \ln P + 389.2$$

where  $T$  is in kelvins and  $P$  is in gigapascals. At 298 K, the calculated freezing pressure is 0.40 GPa. The liquid phase is easily superpressed with the metastable liquid existing to about 2 GPa before rapid crystallization to a polycrystalline phase occurs. The structure of the orthorhombic high pressure phase (space group  $P2_12_12_1$ ) is the same as the structure of the phase that crystallizes at low temperatures and 1 atm.<sup>9,10</sup> No data are shown beyond 1.54 GPa and 433 K because the nitromethane begins to decompose above these conditions. It is not known whether only the liquid or the solid or both phases undergo decomposition at these conditions. Figure 3 shows the infrared absorption spectrum of nitromethane and its thermal decomposition product(s) for the  $1500\text{--}750\text{-cm}^{-1}$  spectral range, which is the region of interest for the kinetic studies. The infrared absorption spectrum of the reaction product(s) had been tentatively identified with either ammonium oxalate or along with traces of HCN,  $N_2O$ ,  $H_2O$ , and possibly  $CO_2$ .<sup>8</sup> In the present experiments mass spectral analysis

positively identifies the major products of the decomposition as ammonia and formic acid or its salt with water also being present. The product was originally reported to be the oxalate salt on the basis of the similarity of the infrared absorption patterns, but that analysis had never been confirmed.<sup>8</sup> The product of the slow thermal decomposition reaction appears to be present in all runs made here up to 7 GPa as shown by the similarity in all spectra obtained for the reaction product(s). Pressure tends to increase the chemical reactivity of nitromethane as well as the rate of thermal decomposition. It was observed, quite accidentally, that a pressure-induced spontaneous explosion of single crystals of nitromethane at ambient temperature can occur. Further study revealed that single crystals grown from the liquid with the 111 and either the 001 or the 100 crystal faces perpendicular to the applied load direction in the DAC, if pressed rapidly to over 3 GPa, exploded instantaneously accompanied by an audible snapping sound similar to that heard when a diamond anvil fails catastrophically under high loads. The normally transparent sample instantaneously becomes opaque when the phenomenon is viewed through the polarizing microscopy. X-ray analysis and also visual examination of the sample revealed an amorphous dark-brown solid residue which when heated is stable to  $>573$  K. Mass spectral analysis of the residue was inconclusive because no well-defined spectra were observed. After the run, black particles remained in the crucible, indicating that much of the material did not volatilize in the spectrometer. Because most of the sample is recovered after the experiment suggests that the residue may be in the form of carbon. However, this conclusion has not been substantiated. We do know that the residue was not ammonium formate, which is the characteristic product for the slow decomposition reaction. It should also be noted that this stress-induced explosion occurs only in the nitromethane because similar experiments on deuterated nitromethane at ambient temperature did not produce the explosion phenomenon.

Previously reported shock experiments on oriented pentaerythritol (PETN) crystals have shown similar type behavior.<sup>12</sup> It was suggested that the sensitivity of shock pressures to orientation is the result of the availability of slip planes or systems of planes in the crystal to absorb the shock thereby increasing the threshold to explosion. A similar explanation may be applicable to the nitromethane crystals as well. The deuteration effect, no doubt, plays a role in the initiation chemistry. An isotope effect has been observed previously in the sensitivity of RDX and HMX to shock and thermal conditions.<sup>13</sup> Thermal explosion times for nitromethane and deuterated nitromethane have been measured as a function of temperature and pressure and also demonstrate an isotope effect.<sup>14</sup> At 1.0 GPa and 546 K, the thermal explosion time for the deuterated species was found to be 10 times larger than that for nitromethane. As far as we know, no determination of the crystal structure of deuterated nitromethane at high pressure has been reported. However, measurements on the energy levels of the rotational modes of the  $CH_3$  and  $CD_3$  groups in nitromethane have been made at 0.5 GPa by neutron inelastic scattering.<sup>15,16</sup> The results of those measurements suggest that the crystal structures of the deuterated and protonated species are the same.<sup>16</sup>

*Kinetic Data.* Unlike RDX and HMX, where as many as nine vibrational bands can be used to investigate the effects of pressure and temperature on their decomposition rate without interference from absorption bands arising from reaction products, nitromethane decomposition results in a reaction product spectrum that interferes with most of the major vibrational bands of the reacting sample. Only the bands at  $1100$  ( $\nu\text{-CH}_3$ ) and  $925\text{ cm}^{-1}$  ( $\nu\text{-CN}$ ) (assignments indicated can be found in ref 7 and 8) are useful

(12) Dick, J. J. *Appl. Phys. Lett.* **1984**, *44*, 859.

(13) Balusu, S.; Weinstein, D. I.; Autera, J. R.; Velicky, R. W. *J. Phys. Chem.* **1986**, *90*, 4121.

(14) Shaw, R.; DeCarli, P. S.; Ross, D. S.; Lee, E. L.; Stromberg, H. D. *Combust. Flame* **1979**, *35*, 237.

(15) Trevino, S. F.; Rymes, W. H. *J. Chem. Phys.* **1980**, *73*, 3001.

(16) Cavagnat, D.; Magerl, A.; Vettier, C.; Anderson, I. S.; Trevino, S. F. *Phys. Rev. Lett.* **1985**, *54*, 193.

(7) Malewski, G.; Pfeiffer, M.; Reich, P. *J. Mol. Struct.* **1969**, *3*, 419.

(8) Holman, M.; Pinchas, S. *J. Chem. Soc.* **1960**, 1246.

(9) Cromer, D. T.; Ryan, R. R.; Schiferl, D. *J. Phys. Chem.* **1985**, 2315.

(10) Trevino, S. F.; Prince, E.; Hubbard, C. R. *J. Chem. Phys.* **1980**, *76*, 2996.

(11) Brasch, J. W. *J. Phys. Chem.* **1980**, *84*, 2084.

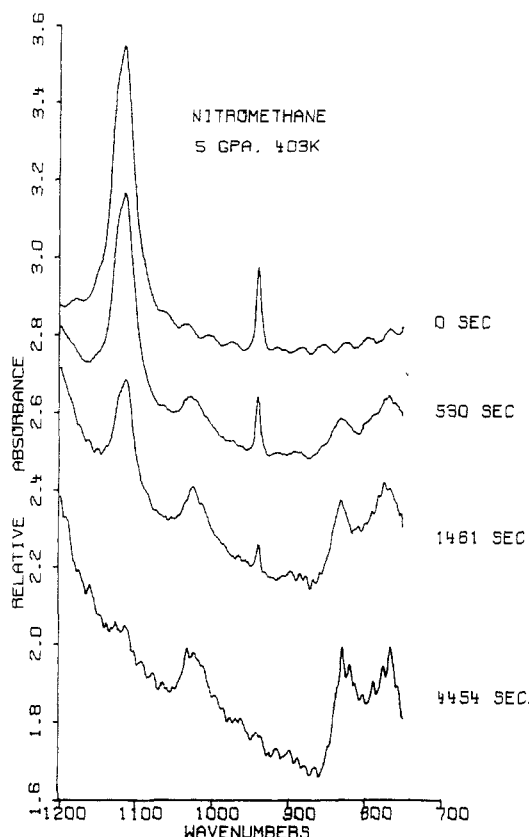


**Figure 4.** Infrared absorbance spectra of nitromethane at 5.0 GPa and 403 K for several times during thermal decomposition. Spectra such as these are typical of our measurements over the pressure-temperature domain studied. Only the two peaks shown here at 1100 and 925  $\text{cm}^{-1}$ , which are due solely to vibrational frequencies of modes in crystalline nitromethane, were used in the analysis of the data. All other bands in the spectrum were unsuitable for the analysis because they exhibited interference either from other bands of nitromethane or from bands arising from the products of decomposition. Time  $t = 0$  indicates the time at which sample temperature reached decomposition temperature. The spectrum at 4454 s shows no nitromethane bands and only those from the products of thermal decomposition.

for the kinetic analysis as can be seen in Figure 4. Typical spectra for these two absorption bands of nitromethane reacted at 5.0 GPa and 403 K for various times during the decomposition reaction are shown in Figure 4. At time  $t = 0$ , the sample temperature reached the desired decomposition temperature. Measurements of this type were made over the temperature range 393–453 K in 10 K increments and over the pressure range 2.0–7.1 GPa. Not all combinations possible in this pressure-temperature regime were studied, though. The following results were obtained.

The concentration of nitromethane is proportional to the measured absorbance. The fraction of nitromethane remaining as the reaction proceeds is expressed as  $\alpha$ . This is obtained by taking ratios of the peak absorbencies normalized to zero at time zero. Ratios were determined for the two peaks and were combined to give an average value, which was then subtracted from unity to yield  $\alpha$ , a term proportional to the mole fraction of nitromethane reacted.  $\alpha$ ,  $(1 - \alpha)$ , and  $\ln(1 - \alpha)$  are then plotted as a function of time for the various pressures and temperatures studied. The resulting curves and dependencies on time can tell us something about the kind of mechanism involved in the decomposition reaction.

Typical  $\alpha$  vs time curves for data obtained at 2 GPa and for temperatures of 403, 413, and 423 K are shown in Figure 5. For the lower two temperatures,  $\alpha$  does not appear to be a linear function of time, nor do they follow any of the other common kinetic laws. As in the case of HMX, these curves can be identified with the initial and intermediate stages of a sigmoid (*s* shaped)  $\alpha$  vs time curve characteristic of thermal decomposition of a single solid in an autocatalytic type reaction.<sup>1</sup> As temperature is in-

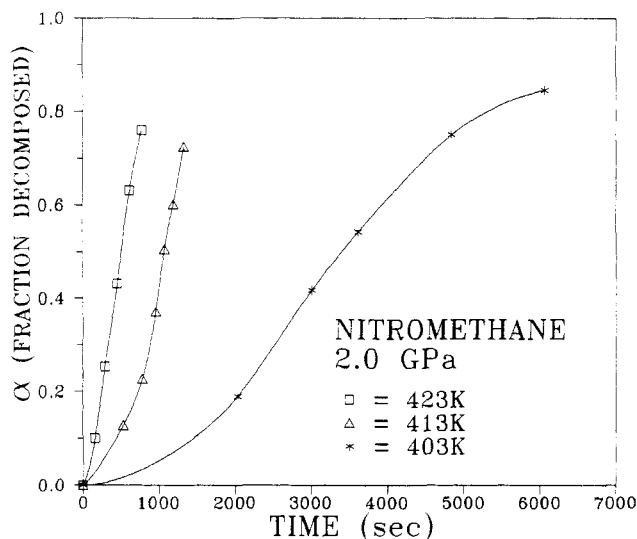


**Figure 5.**  $\alpha$  vs time sigmoid-type curves for data obtained at 2.0 GPa for the temperatures indicated.  $\alpha$  is the fraction of decomposed nitromethane at time,  $t$ , during thermal decomposition. Curves shown are logarithmic fits to the data points.

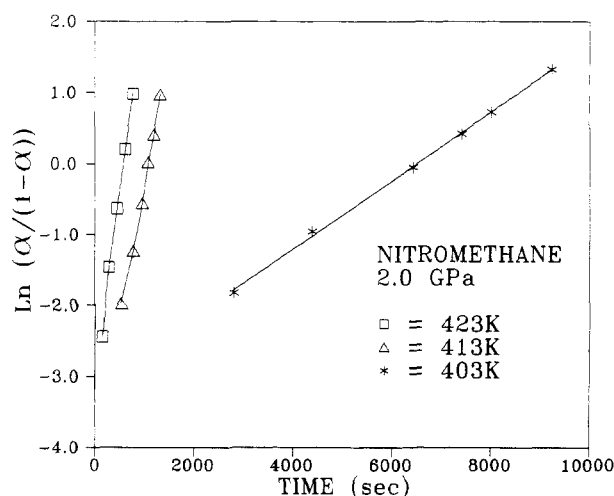


**Figure 6.** Linear fits of  $\ln[\alpha/(1 - \alpha)]$  vs time for data obtained at 2.0 GPa for the decomposition temperatures indicated. The overall decomposition rate increases with increasing temperature, typical Arrhenius behavior.

creased the *s* character diminishes to where the curve is almost linear at 423 K. Since the time required for the sample to reach the decomposition temperature is relatively short compared to the time necessary for the reaction to go to completion, the small differences found in some cases between  $t = 0$  and  $\alpha = 0$  have no significant effect on the shape of these curves. For this set of sigmoid-type curves, a plot of  $\ln[\alpha/(1 - \alpha)]$  vs time gives linear dependencies as indicated in Figure 6. Linearity of the fit supports a decomposition mechanism that consists of nuclei formation with branching interference. The slopes of these lines give typical Arrhenius temperature behavior with the overall rate increasing with increasing temperature at a constant pressure of 2.0 GPa.

This type of dependence was found for the thermal decomposition of HMX in our earlier work,<sup>1</sup> where the results turned out to be more consistent than in the present case. Unlike HMX, where the general shape of these curves remained essentially unchanged over the 3.0–6.5-GPa range studied, nitromethane appears to undergo significant changes in its reaction mechanism. For example, above 413 K, the general shape of the  $\alpha$  vs time curves changes. It was also found that at pressures greater than 5 GPa a third change in the reaction mechanism, as indicated by a change in the shape of the  $\alpha$  vs time curve, is observed. Because we can use only two absorbance bands which have large inherent signal-to-noise error to calculate the nitromethane concentration

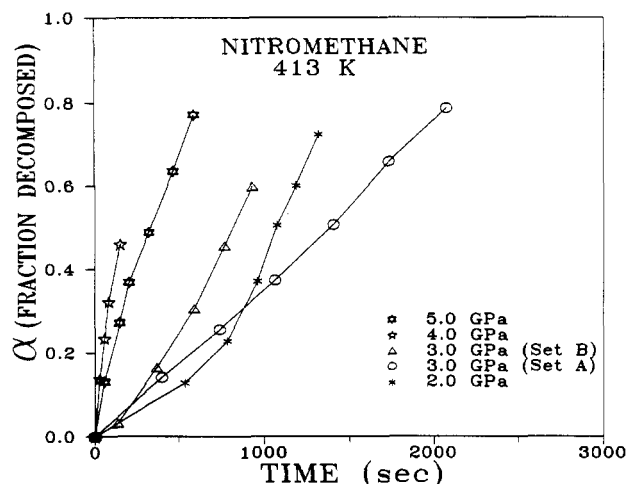


**Figure 7.**  $\alpha$  vs time plots as a function of pressure for the thermal decomposition of nitromethane at a constant temperature of 413 K. The observed pressure dependence does not show a consistent trend. The expected fastest rate should be for the data taken at 5.0 GPa. Instead, the 4.0-GPa data give the fastest rate. The slowest rate initially is the 2.0-GPa data, but with time it overtakes the 3.0-GPa data (set A).

term,  $\alpha$ , and also because multiple reaction mechanisms appear to overlap in the pressure-temperature regime studied, a precise quantitative analysis of the data is not possible as demonstrated by the results shown in Figure 7. However, there are some interesting qualitative observations that can be made on the basis of reaction times at various pressure-temperature regimes:

(1) To 5 GPa at least two different reaction mechanisms are involved in the decomposition and both have a positive pressure dependence on the overall rate of thermal decomposition.

(2) Mechanism 1 is dominant below 4 GPa and  $T \leq 403$  K.

(3) Mechanism 2 operates at all measured temperatures at 5 GPa and at  $T \geq 413$  K at 4 GPa.

(4) The mechanism crossover temperature appears to be 413 K. At  $T \leq 413$  K at 2 GPa mechanism 1 is operative, but at  $T \geq 413$  K either mechanism 2 or a mixture of both are operative.

(5) Mechanism 1 is linearly dependent in  $\ln[\alpha/(1-\alpha)]$  vs time, similar to that found earlier for  $\beta$ -HMX, while mechanism 2 is linear in  $\ln(1-\alpha)$  vs time. The mathematical functionality of  $\alpha$  with respect to time determines the type of predominant chemical mechanism of the decomposition reaction.<sup>5</sup> The fact that we find two different time dependencies as shown in Figures 6 and 8 indicates that we are dealing with two separate and distinct kinetic processes. Recently, it was reported that the aci or enol form of nitromethane can play an important role in the thermal decomposition of nitromethane by acting as a catalyst.<sup>17</sup> The results obtained here cannot rule out the possibility of the enol form affecting our observed kinetic data.

(6) Finally, a third mechanism operates at pressures greater than 5 GPa.

The results of this study show clearly the complexity of the nitromethane thermal decomposition reaction. More than one kinetic mechanism and/or catalytic effect may be present. However, the results show definitely a positive pressure enhancement of the reaction rate. As described in ref 1, the total differential of the natural logarithm of the reaction rate is given as

$$d \ln k = \Delta H^*/RT^2 dT - \Delta V^*/RT dP$$

For small increases in pressure with all other terms being equal, only a negative  $\Delta V^*$  will cause increases in  $\ln k$ . Therefore, the thermal decomposition rate of nitromethane shows a negative volume of activation in the pressure-temperature regime studied in the present experiments. This result directly implies that the nitromethane decomposition reaction in the solid state is bimolecular in character.

(17) Engelke, R.; Earl, W. L.; Rohlfling, C. M. *J. Phys. Chem.* **1986**, *90*, 545.

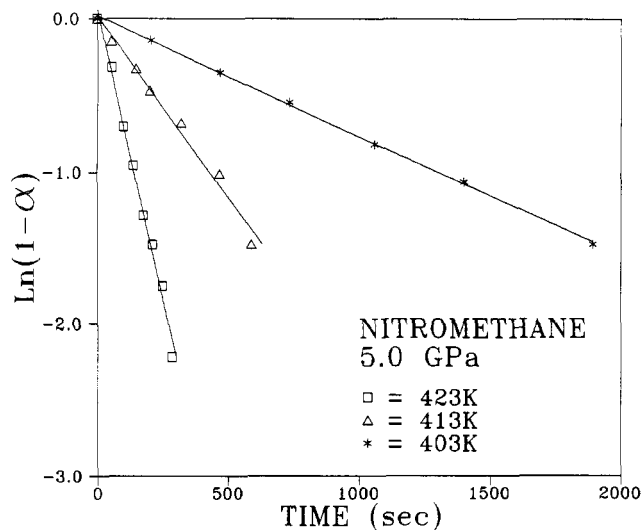
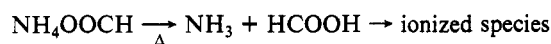


**Figure 8.** Linear fits of  $\ln(1-\alpha)$  vs time for data obtained at 5.0 GPa at three decomposition temperatures. The linearity in the fit indicates a reaction mechanism different from the one found for the data plotted in Figure 6.

lecular in character. This result contradicts recent mass spectra studies of molecular reactions in the gas phase,<sup>18-20</sup> where the reaction is found to be unimolecular. This disagreement in the results is not surprising because different decomposition mechanisms can be expected between the crystalline and gaseous phases of nitromethane.

Mass spectra analysis of the products resulting from nitromethane reacted at 473 K and 1.8 GPa for 1 h and retrieved to ambient conditions of pressure and temperature gave the following results. At probe temperatures of 423-453 K, a strong signal was recorded that is consistent with ammonium formate. Intense ions at  $m/z$  17 and 46 are characteristic of ammonia and formic acid, respectively. These two compounds are the expected products of the thermal decomposition of ammonium formate. A strong signal for water was also recorded, but the background also exhibits a strong water signal, so that the relative amount of water in the reaction products cannot be determined. Another complicating feature is the fact that ammonium formate is hygroscopic so that the origin of the water signal becomes even more obscured. The other strong ions observed are consistent with fragment ions for ammonia and formic acid. They are at  $m/z$  44 and 45. The relative abundances of  $m/z$  44, 45, and 46 are very close to the reference spectrum in the NIH/EPA data base for formic acid, thus any oxalate ion would necessarily be at very low levels. The mass spectroscopic technique used here permits only analysis of the final stable form of the thermally heated species, for which the following reactions apply:



**Chemical Mechanism.** Considerable work has been reported on the possible chemical reaction pathways for both pyrolysis and detonation processes in nitromethane.<sup>18-22</sup> In general, most of these pathways are based on the results of mass spectral analysis. Furthermore, most of these proposed mechanisms are based upon a unimolecular process. As far as we can determine, only this work and one other (see ref 2) show experimentally that the reaction under pressure results from a bimolecular process, al-

(18) Dewar, M. J. S.; Ritchie, J. P.; Alster, J. *J. Org. Chem.* **1985**, *50*, 1031.

(19) Wodtke, A. M.; Hints, E. J.; Lee, Y. T. *J. Chem. Phys.* **1986**, *84*, 1044.

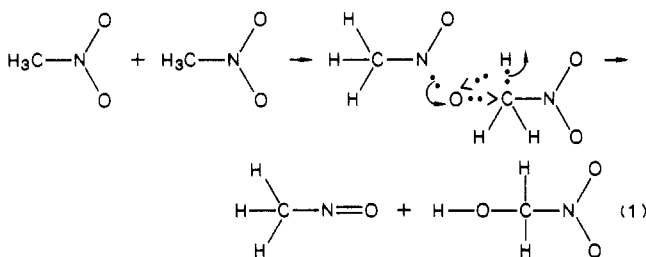
(20) Bardo, R. D. In *Proceedings of the Eighth Symposium (Int.) on Detonation*, NSWC MP 86-194, NSWC White Oak, Silver Spring, MD 20903-5000, Albuquerque, NM, July 15, 1985.

(21) Brower, K., private communication.

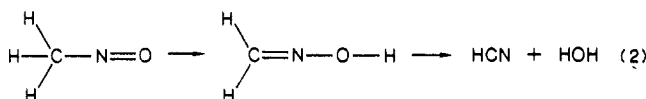
(22) Schroeder, M. A. Technical Report BRL-TR-2659, U.S. Army Ballistic Research Laboratory, Aberdeen Proving Ground, MD, June 1985.

though the results reported in ref 2 were derived from the effect of pressure on time-to-explosion measurements.

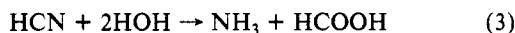
On the basis of theoretical electronic orbital calculations a bimolecular process has been proposed<sup>20</sup> as follows:



The quantum mechanical calculations show this to be a three-center reaction complex, where, under high pressure, the potential surface contacts result in a simultaneous motion of atoms, as indicated by the arrows, to form the resultant products. The reaction of the nitrosomethane rapidly proceeds to form HCN and finally  $\text{NH}_3$  and  $\text{HCOOH}$ :



At elevated pressure and temperature, HCN hydrolyzes very fast:



The remaining product from reaction 1 rapidly decomposes (reaction 4) into the following possible gaseous compounds:  $\text{H}_2\text{O}$ ,  $\text{N}_2\text{O}$ ,  $\text{CO}_2$ ,  $\text{CO}$ ,  $\text{NO}$ ,  $\text{H}_2$ , and  $\text{C}(\text{s})$ .

Reaction 1 is rate controlling with a calculated activation energy of  $32.5 \text{ kcal mol}^{-1}$ . Reactions 2-4 are relatively fast compared with reaction 1. Reactions 3 and 4 provide the pathways for the production of  $\text{NH}_3$ ,  $\text{HCOOH}$ , and  $\text{H}_2\text{O}$  via chemical reaction with HCN, which is known to be a major pyrolysis product of nitromethane.<sup>21</sup> Our experiments confirm the presence of  $\text{NH}_3$ ,  $\text{HCOOH}$ , and  $\text{H}_2\text{O}$  along with volatile gases as the major products of thermal decomposition of nitromethane under high pressures.

While it is true that other mechanisms can result in a positive pressure dependence on the rate of a reaction, in the case of

nitromethane decomposition, our measured effects and experimentally identified reaction products provide strong evidence to support the theoretically proposed mechanism.<sup>20</sup> This conclusion, however, is not unequivocal.

This proposed reaction scheme for nitromethane decomposition at elevated pressures suggests a strong intermolecular interaction of nitromethane in the condensed phase. If this is indeed the case, then it is important to investigate the effect of pressure on the vibrational bands in nitromethane and to analyze the observed shifts in light of intermolecular coupling between the  $\text{NO}_2$  and  $\text{H}_3\text{C}$  groups of interacting molecules. This is the subject of the succeeding article in this journal issue.

## Conclusions

Nitromethane thermally decomposes under pressure when heated to temperatures above 440 K at pressures greater than 1.6 GPa. Both pressure and temperature accelerate the rate of thermal decomposition. The condensed product residues are mainly ammonium formate and water in addition to nonretrievable volatile gases. More than one decomposition mechanism or catalytic effect appears to be present as indicated by the complex kinetic results. A proposed bimolecular mechanism is presented that can account for the observed positive pressure dependence of the reaction rate and the experimentally detected reaction products. Nitromethane also was observed to undergo a catastrophic reaction under certain dynamic stress conditions in the DAC at room temperature. The sensitivity level to this catastrophic reaction appears to be crystal orientation dependent with respect to the applied stress in the DAC. The resulting solid residue from this reaction is amorphous and carbonaceous in character, stable to temperatures in excess of 573 K. Under the same conditions, deuteriated nitromethane did not undergo the catastrophic reaction.

*Acknowledgment.* We thank S. Trevino (NBS) for providing the protonated and deuteriated samples of nitromethane, M. J. Welch (NBS) for carrying out the mass spectrometry measurements, and B. Fanconi (NBS) for helpful assistance with the FTIR instrument. We also acknowledge the U.S. Army Research Office and the Naval Surface Warfare Center, Independent Research Program, for financial support for this project.

Registry No. Nitromethane, 75-52-5.

## Effects of Pressure on the Vibrational Spectra of Liquid Nitromethane

P. J. Miller,\*

Naval Surface Warfare Center, White Oak, Maryland 20910

S. Block, and G. J. Piermarini

Institute for Materials Science and Engineering, National Bureau of Standards, Gaithersburg, Maryland 20899 (Received: January 15, 1988; In Final Form: June 22, 1988)

A complete normal-coordinate calculation for nitromethane is given using the vibrational frequencies measured from the three isotopes  $\text{CH}_3\text{NO}_2$ ,  $\text{CD}_3\text{NO}_2$ , and  $\text{CH}_3^{15}\text{NO}_2$ . Pressure effects on the vibrational normal modes of the superpressed liquid to 2.0 GPa also were measured. A softening of the frequency of the asymmetric stretching mode of  $\text{NO}_2$  with increasing pressure indicated a strong intermolecular interaction. By calculating a minimum energy pair configuration and applying two-site exciton theory, we calculated the shifts of the normal modes of the  $\text{NO}_2$  stretching vibrations as a function of density and pressure and found them to agree qualitatively with the experimentally measured shifts. The results support the bimolecular nature of the mechanism for the thermal decomposition of nitromethane under pressure.

## Introduction

In a related paper on the effects of pressure on the thermal decomposition kinetics and chemical reactivity of nitromethane, we showed that nitromethane thermally decomposed under pressure through a complex bimolecular mechanism.<sup>1</sup> A de-

composition mechanism was proposed for this reaction that explains both its bimolecular nature and the observed reaction

(1) Piermarini, G. J.; Block, S.; Miller, P. J. *J. Phys. Chem.*, preceding paper in this issue.